Asteroids, Comets, Meteors 1991, pp. 583-586
Lunar and Planetary Institute, Houston, 1992

S136-70

N93-19249

CARTOGRAPHY OF ASTEROIDS AND COMET NUCLEI FROM LOW RESOLUTION DATA

Philip J. Stooke
Department of Geography, University of Western Ontario
London, Ontario, Canada N6A 5C2 (Stooke@vaxr.sscl.uwo.ca).

High resolution images of non-spherical objects, such as Viking images of Phobos and the anticipated Galileo images of Gaspra, lend themselves to conventional planetary cartographic procedures: control network analysis, stereophotogrammetry, image mosaicking in 2D or 3D and airbrush mapping (1). There remains the problem of a suitable map projection for bodies which are extremely elongated or irregular in shape. Many bodies will soon be seen at lower resolution (5 - 30 pixels across the disk) in images from speckle interferometry, the Hubble Space Telescope (even after repair), ground-based radar, distant spacecraft encounters and closer images degraded by smear. Different data with similar effective resolutions are available from stellar occultations, radar or lightcurve convex hulls, lightcurve modelling of albedo variations and cometary jet modelling. With such low resolution, conventional methods of shape determination will be less useful or will fail altogether, leaving limb and terminator topography as the principal sources of topographic information.

I have developed a method for shape determination based on limb and terminator topography (2,3,4,5). It has been applied to the nucleus of Comet Halley (6) and the jovian satellite Amalthea (7). The Halley map will be repeated now that a new consensus appears to be emerging on the nucleus rotation state. The Amalthea results are described here to give an example of the cartographic possibilities and problems of anticipated data sets.

Voyager images of Amalthea were decompressed from PDS CD-ROMs, outlines digitized and coordinates converted to kilometres in the image plane. An initial triaxial ellipsoid model was registered with the digitized outlines and iteratively modified by locally increasing or decreasing radii until the model successfully duplicated all limbs and terminators in the eight images used for modelling. Topography of major craters and ridges was estimated but is very poorly constrained by the data. For instance, the depths of the two largest craters on Amalthea are virtually unknown. The model is illustrated with graticules depicting Voyager images (Figure 1), and views from mutually perpendicular directions including the polar view not seen by Voyager (Figure 2).

The origin of the planetocentric coordinate system is the assumed centre of mass, tested by comparing volumes on either side of three mutually perpendicular planes during modelling. The centre of mass is probably within about 5 km of the position assumed here, assuming uniform or radially symmetrical internal mass distribution. The model has a volume of 2.5 $\pm$ 0.5 million cubic km. Radii are typically uncertain by about 2 pixels (10 to 20 km) near limbs and terminators (less where several intersect), but are very poorly constrained elsewhere. Although limbs can be located to within a pixel on most Voyager images, their geographic locations on the model are uncertain by many degrees, a major source of uncertainty in the model and very difficult to quantify.

Cartographic options for non-spherical worlds have until recently been very limited. The first such maps (e.g. 8,9), rough sketches on unmodified cylindrical projections of a sphere, inevitably contain enormous distortions. More sophisticated approaches include a modified cylindrical (Mercator-like) projection developed by John Snyder (10) and so far used only for a Soviet map of Phobos, and the use of mutually perpendicular orthographic views of a 3-D digital photomosaic (11). These suffer from other problems. The cylindrical projections give a good representation of the circumequatorial regions with relatively minor distortions if the body is well approximated by a triaxial ellipsoid. They will contain massive distortions if the shape is more complex and do nothing to indicate the true shape of the body. The orthographic approach suffers mainly from excessive redundancy since six orthogonal views are needed for good surface coverage. That number could increase for bizarre shapes such as toroidal or pretzel-like pierced forms which might result from prolonged deepening of active vents on comet nuclei. Bodies with a distinctly faceted shape, with roughly planar faces forming a shape more like a pyramid than a cube, might suffer from this approach if axis-fixed orthogonal views were always significantly oblique to one or more faces.

I have described a map projection system based on azimuthal projections in which the radius constant of the spherical projection is replaced with the local radius of the surface to be projected (2,3,4,5), ultimately inspired by the work of Ralph Turner (12). Any azimuthal projection can be modified in this way, giving as a minimum equal area, equidistant and conformal versions (Figure 3). The conformal version is the equivalent of the familiar Stereographic projection. For maps of a body divided into two 'hemispheres' the boundary of each half exactly reproduces the cross-sectional shape in the dividing plane, giving a good idea of the true shape and positions of features relative to that shape. Parallels and meridians follow topography and act as 'form lines', enhancing shape visualization. Because of these qualities this class of projection is called morphographic. Distortions are very much less severe in these maps than in unmodified cylindrical projections (4,5) and are minimized for an elongated object if maps of opposite 'hemispheres' are centred on the shorter axes rather than the longest.

In work undertaken to date (6,7) the projection has been applied to the actual shape of the body, so far as it can be determined by the modelling approach described above. This works well for bodies which correspond

reasonably well to a triaxial ellipsoid shape, with small craters or hills but no massive deviations from the smooth surface. It is less satisfactory in cases where a major concavity exists, such as the south polar 'saddle' of Deimos or the large and deep craters Pan and Gaea on Amalthea. The principal problem is that these projections are not 'unique'. A point's location is determined both by its angular distance from the origin of the projection and by the radius at that point. Along a single azimuth from the origin, two points with certain combinations of radius and angular distance may coincide. This is most severe when areas of high local relief occur near the boundary of the 'hemisphere'. A high ridge or crater wall may be projected outwards from the centre of the map to overlie a more distant depression, a phenomenon resembling layover in synthetic aperture radar (SAR) images. In lower relief areas crater bottoms are displaced towards the centre of the map by an amount related to angular distance from the centre of the map, and hilltops are displaced outwards, again similar to distortions in SAR images.

The 'layover' problem can be reduced by selecting a different morphographic projection. The conformal projection expands the outer part of each 'hemisphere' more than the equal area version, and reduces the effect, but this limits choice of projection. It is preferable to apply the desired projection to a different surface than the actual topography of the body. There are several possibilities. The simplest is to use the best fit triaxial ellipsoid as a projection surface. Topography is projected onto the triaxial ellipsoid along ellipsoid radii, and the ellipsoid is then projected according to the morphographic equations. This works well to give an impression of the degree of elongation of the body and the positions of features relative to the overall shape. Where the shape is poorly determined (e.g. speckle or HST images of asteroids with about 10 pixels across the disk) but substantial elongation is apparent this is probably the most desirable form of the projection to use. A better indication of overall shape can be obtained by using the three dimensional convex hull of the body as a projection surface. The global shape will be still better depicted if the projection is applied to the surface on which craters and steep hills or ridges are superimposed. This is obtained by extending the local surface across craters to roughly duplicate the pre-impact topography of the region, and by removing the most prominent hills and ridges. The largest concavities (e.g. south polar saddle of Deimos) would remain, but localized high relief would be smoothed over on the projected surface. The relief is removed from the surface which controls the projection, but would be portrayed on the map as a photomosaic or by contouring or relief shading. Various versions of a map grid for Amalthea illustrate this (Figure 4). The triaxial ellipsoid model is composite: the longest semi-axes are 150 km away from Jupiter and 120 km towards Jupiter. The **b** and **c** semi-axes are 75 and 70 km respectively. All grids in Figure 4 are conformal.

The shape-modelling method described above can be applied to any object for which low resolution data are acquired. The morphographic map projections are suitable for all non-spherical bodies including those whose shapes are more precisely known. Particularly significant uses include registering data obtained by different techniques (e.g. HST images and a radar convex hull) or at different oppositions (e.g. HST images of an asteroid centred at two different latitudes), and estimating local slopes to help interpret disk-resolved photometry. The results can be portrayed graphically as shown here, giving base maps for geological interpretation and aids to visualization of the object itself. To illustrate mapping options I present a shaded relief map of Amalthea with local radius contours (Figure 5) and an albedo province map of asteroid (4) Vesta (Figure 6). The Vesta map assumes the triaxial ellipsoid shape described by Drummond et al. (13), though a spherical form is probably preferable. The projection gives an equal area map of the triaxial ellipsoid. The albedo patterns are a composite of speckle images (13), lightcurve modelling (14) and rotational spectral variations (15). The letter labels are from ref. (13). This map is intended only to illustrate the projection and should not be interpreted as a definitive model of the albedo distribution on (4) Vesta.

REFERENCES: **(1)** Greeley R., Batson R.M., eds (1990) Planetary Mapping. Cambridge University Press. **(2)** Stooke P.J. (1986) Automated cartography of non-spherical worlds. Proc. 2nd Internat. Symp. Spatial Data Handling, pp. 523-536. **(3)** Stooke P.J., Keller C.P. (1987) Morphographic projections for maps of non-spherical worlds. Lunar Planet. Sci. XVIII, pp. 956-957. Lunar and Planetary Institute, Houston. **(4)** Stooke P.J. (1988) Cartography of Non-Spherical Worlds. Ph.D. Diss., Univ. of Victoria. 169 pp. **(5)** Stooke P.J., Keller C.P. (1990) Map projections for non-spherical worlds - the variable radius projections. Cartographica 27 (2), 82-100. **(6)** Stooke P.J., Abergel A. (1991) Morphology of the nucleus of comet P/Halley. Astron. Astrophys. (in press). **(7)** Stooke P.J. (1991) A model and map of Amalthea. Earth, Moon, Planets (in press). **(8)** Duxbury T.C. (1974) Phobos: control network analysis. Icarus 23, 290-299. **(9)** Veverka J., Thomas P., Davies M., Morrison D. (1981) Amalthea: Voyager imaging results. Journ. Geophys. Res. 86, 8675-8692. **(10)** Snyder J.P. (1985) Conformal mapping of the triaxial ellipsoid. Survey Review 28, 130-148. **(11)** Planetary Cartography Working Group (1984) Planetary Cartography in the Next Decade (1984-1994). NASA SP-475, National Aeronautics and Space Administration, Washington D.C. **(12)** Turner R. (1978) A model of Phobos. Icarus 33, 116-140. **(13)** Drummond J., Eckart A., Hege E.K. (1988) Speckle interferometry of asteroids. IV. Reconstructed images of 4 Vesta. Icarus 73, 1-14. **(14)** Cellino A., Zappala V., Di Martino M., Farinella P., Paolicchi P. (1987) Flattening, pole, and albedo features of 4 Vesta from photometric data. Icarus 70, 546-565. **(15)** Gaffey M.J. (1983) The asteroid (4) Vesta: rotational spectral variations, surface material heterogeneity, and implications for the origins of the basaltic achondrites. Lunar Planet. Sci. XIV, pp. 231-232. Lunar and Planetary Institute, Houston.

Figure 1.
Amalthea model, orthographic views matching Voyager images.

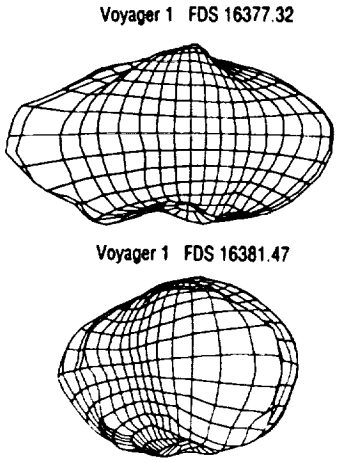

Figure 2.
Orthographic orthogonal views of the Amalthea model.

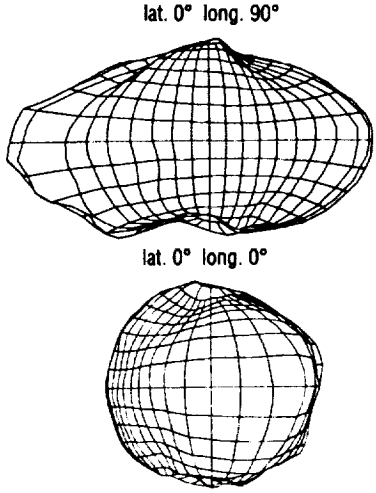

Figure 3.
Equal area (top) and conformal map grids for Amalthea.

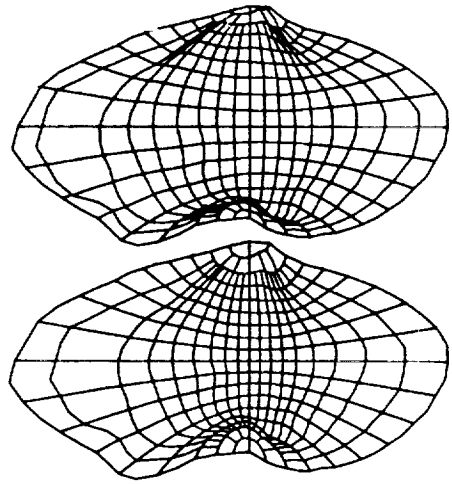

Figure 4.
Conformal map grids for one side of Amalthea, based on the best-fit triaxial ellipsoid model (see text) (left), convex hull of the topographic model (centre) and full topographic model (right). Grid on left is distorted by mismatch of true and model shape, grid on right by 'layover' on the rim of crater Gaea at the south pole.

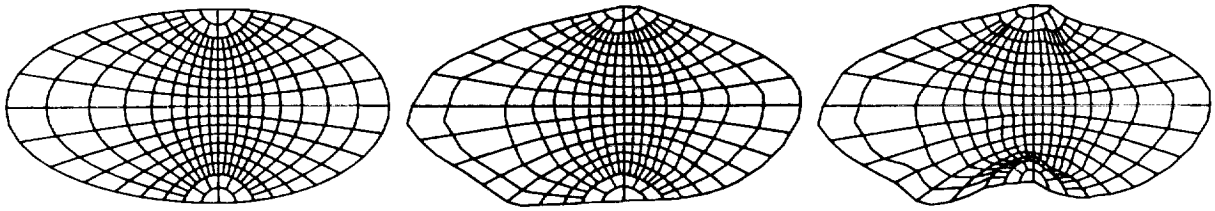

Figure 5.
Shaded relief map of Amalthea, morphographic conformal projection, with radius contours at 10 km intervals.

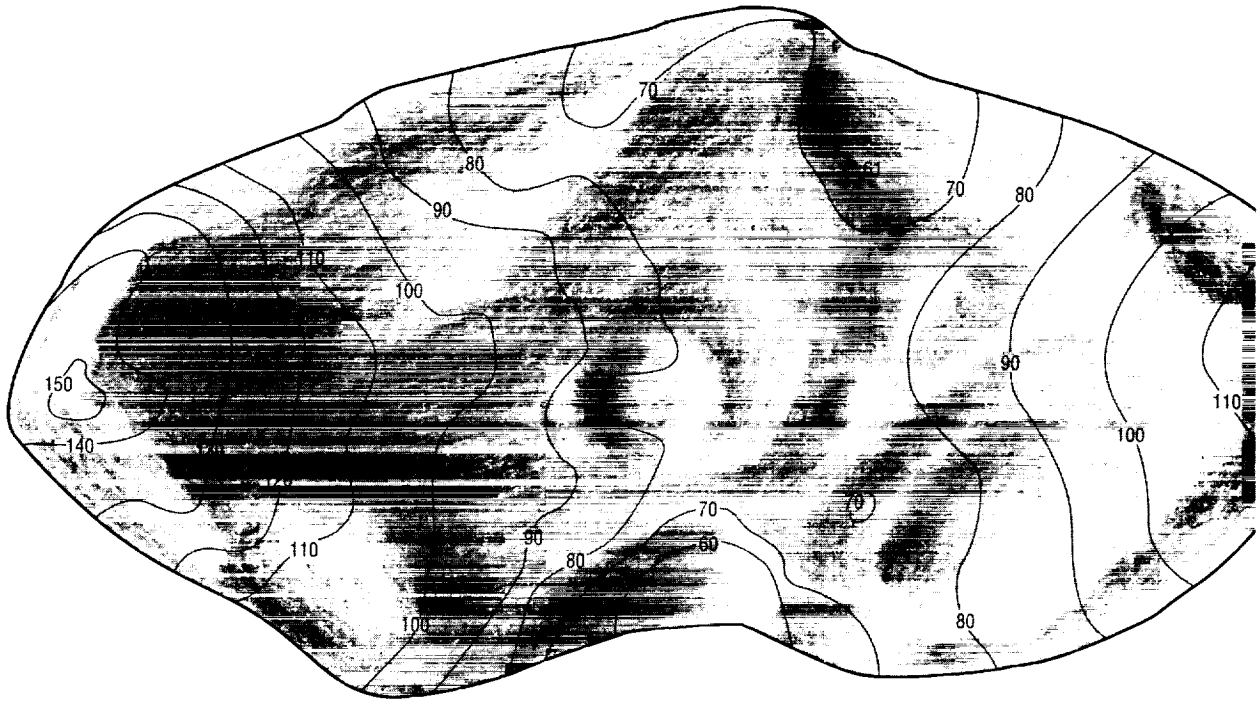

Figure 6.
Albedo provinces on asteroid (4) Vesta based on refs. 13,14,15. This is intended only to illustrate the projection, an equal area map of a triaxial ellipsoid (dimensions from ref. 13), not to be a definitive model of the shape or surface markings of Vesta.